RSC Advances

PAPER

View Article Online
View Journal | View Issue

Cite this: *RSC Adv.*, 2018, **8**, 24641

A model study on the photodecarbonyl reaction of $(\eta^5\text{-}C_5H_5)M(CO)_2$ (M = Co, Rh, Ir)†

Zheng-Feng Zhang[a] and Ming-Der Su *[ab]

Received 6th May 2018
Accepted 15th June 2018

DOI: 10.1039/c8ra03866j

rsc.li/rsc-advances

The group 9 organometallic complexes η^5-CpM$(CO)_2$ (M = Co, Rh, and Ir) and $Si(CH_3)_3(H)$ have been considered as a model system to study their photochemical decarbonyl reactions as well as the Si–H bond activation reactions using the CASSCF and MP2-CAS computational methods. For the cobalt complex, three kinds of reaction pathways, which result in the same oxidative addition product, are investigated. Our theoretical finding demonstrated that after the photoirradiation, η^5-CpCo$(CO)_2$ loses one CO ligand without any difficulty to form either the triplet ($[\eta^5$-CpCo$(CO)]^3$) or singlet ($[\eta^5$-CpCo$(CO)]^1$) species. The former plays a decisive role in the formation of the final oxidative addition product. On the other hand, the latter plays no role in the production of the final product molecule, but its singlet cobalt center interacts weakly with solvent molecules ($(Me_3)SiH$) to produce an alkyl-solvated organometallic complex, which is experimentally detectable. The present works reveal that both η^5-CpRh$(CO)_2$ and η^5-CpIr$(CO)_2$ should adopt the conical intersection mechanism after they are irradiated by light. Moreover, our theoretical examinations strongly suggest that for the 16-electron monocarbonyl η^5-CpM(CO) (M = Rh and Ir) species, the insertion into a Si–H bond by the Ir system is much more facile and more exothermic than that for the Rh counterpart.

I. Introduction

The photochemical oxidative addition reaction of one E–H (E = H or group 14 elements) bonding to the transition metal complex is of essential interest in different fields of chemical research, such as inorganic chemistry, organometallic chemistry, biochemistry, and most importantly, catalytic experimentation,[1–6] ever since the groundbreaking discovery by Schuster-Woldan and Basolo.[7] The basic approach is to break a metal–ligand bond upon coordination by using light to enable subsequent oxidative addition reactions. In this process, one particularly exciting reaction is the photochemical activation of an E–H bond by one unsaturated intermediate CpML (Cp = η^5-C_5H_5) with a 16 valence electron count, which is formed by the two-legged piano stool (half-sandwich) complex $CpML_2$ upon light irradiation.[8–49] Since the CpML complexes can be easily prepared for experiments,[11–14] it is thus not surprising that many experimental and theoretical chemists have investigated either the chemical synthesis or the energy sequences of these intermolecular E–H bond activation reactions.[8–49] Nevertheless, most of the E–H bond insertion reactions by $CpML_2$ organometallic compounds are heavily focused on their thermodynamical aspects, with a few discussions of their initially photochemical aspects. Indeed, to our knowledge, there has been little mechanistic study regarding the photolysis of the $CpML_2$ complex,[24–36] much less related theoretical research. In addition to the limitations of the spectroscopic instruments, there are many fundamental questions about the photolysis of $CpML_2$ in hydrosilane solution that need to be answered. For instance, how does a photo-excited $CpML_2$ molecule go from the excited state to the ground singlet state? And, how does a spin state of the CpML intermediate play a role in its photochemical oxidative addition reactions?.

Theoretical considerations should thus help experimental chemists to gain a better understanding for the mechanisms of the photochemical decarbonylation reactions of the $CpML_2$ complexes. Until now, however, there have been no publications on theoretical interpretations for such photochemical mechanisms.[8–49] The lack of theoretical investigations could be because the sophisticated computational methods for such photochemical reactions studies have not been suitable until recently. In particular, the photochemical activated systems involve transition metal atoms (concerning the spin–orbit coupling). The current work thus undertakes an examination of the mechanisms for the photochemical CO-extrusion reaction of the group 9 d^8 transition metal complex, η^5-CpM$(CO)_2$ (M = Co, Rh, and Ir) as well as its oxidative addition of a Si–H bond in trimethylsilane, eqn (1).

[a]*Department of Applied Chemistry, National Chiayi University, Chiayi 60004, Taiwan*
[b]*Department of Medicinal and Applied Chemistry, Kaohsiung Medical University, Kaohsiung 80708, Taiwan. E-mail: midesu@mail.ncyu.edu.tw*

† Electronic supplementary information (ESI) available. See DOI: 10.1039/c8ra03866j

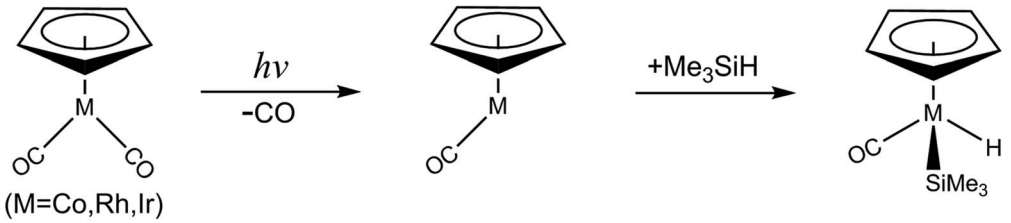

(1)

II. Methodology

Since the photochemical reaction paths involve the singlet ground state as well as the exited singlet and triplet states, the *ab initio* CASSCF (the complete-active-space SCF) program released in GAUSSIAN 09[50] is utilized in the presence of this study. That is, the stationary point structures on the S_0 and S_1 (for **Rea-Rh-S$_0$** and **Rea-Ir-S$_0$** molecules) and the S_0 and T_1 (for **Rea-Co-S$_0$** molecule) potential energy surfaces are investigated at the CASSCF/Def2-SVPD level of computation.[51]

The electronic structure of an organometallic "half-sandwich" complex of the type $CpML_2$ having only 18 electrons in their valence shell has already been discussed elsewhere,[52–54] and is shown in detail in Fig. 1. The active space that needed to properly represent the ground and the lowest excited states of **Rea-Co-S$_0$**, **Rea-Rh-S$_0$**, and **Rea-Ir-S$_0$** contains twelve electrons in eleven (bonding and antibonding metal d) orbitals. That is to say, according to the valence orbitals given in Fig. 1, the active space for the η^5-CpM(CO)$_2$ (M = Co, Rh, and Ir) complex at the singlet ground state can be described as $(\pi_{Cp}/d_{x^2-y^2})^2(\pi_{Cp}/d_{xz})^2(\pi_{Cp}/d_{yz}+p_y)^2(d_{xy})^2(d_{z^2})^2(d_{x^2-y^2})^2$ configuration with five low-lying virtual orbitals $(d_{xz}+p_x/\pi^*_{Cp})^0(\pi^*_{Cp}/d_{yz}+p_y)^0(\pi^*_{Cp}/d_{xz}+p_x)^0(\pi^*_{Cp}/d_{x^2-y^2})^0(\pi^*_{Cp}/d_{xy})^0$. As a consequence, the state-averaged CAS(12,11) mode for the η^5-CpM(CO)$_2$ molecule is applied in the present study to resolve the stationary points on both ground and excited space. In addition, for the oxidative addition reactions, the active space of trimethylsilane is chosen as two electrons in two orbitals, *i.e.*, one bonding σ(Si–H) orbital and one antibonding σ*(Si–H) orbital. As a consequence, the active space for the whole molecular system (η^5-CpM(CO)$_2$ + Si(CH$_3$)$_3$(H)) is referred to as CAS(14,13). For simplicity, in this work, **[Si]^1** stands for trimethylsilane at the singlet state (see below).

Frequency computations based on the CASSCF level of theory for their oxidative addition reactions at the singlet ground state are utilized to examine all points calculated being either minima (the number of imaginary frequencies (NIMAG) = 0) or transition states (NIMAG = 1). The standards for the geometrical optimizations are limited to the maximum force and its root mean square, which are less than 0.00065 and 0.00005 hartree/bohr, respectively. Nevertheless, the computed energies rather than zero-point corrected energies and Gibbs free energies are shown in this work.

Considering the dynamic electron correlations, the multi-reference Møller–Plesset (MP2-CAS) algorithm,[55–65] contained in the GAUSSIAN 09 program package,[43] is carried out. As a result, the relative energies mentioned in this paper are those calculated at the MP2-CAS/Def2-TZVPD level, using the CAS/Def2-SVPD geometry. The active space for each point used in this study is stated above. In consequence, they are abbreviated as MP2-CAS and CAS, respectively. The Cartesian coordinates (CAS) as well as the CAS and MP2-CAS energetics are given in ESI.†

In order to compare the MP2-CAS MP2-CAS singlet-triplet energy difference for the η^5-CpCo(CO)$_2$ complex at different levels of theory, two kinds of density functional theory (DFT) and basis sets are used in this work. That is, B3PW91/Def2-TZVPPD,[66,67] and B3LYP/DZP-DKH.[68,69] The reason for choosing them is because they have been proved to be reliable for examining the relative energetics.[70] Their Cartesian coordinates and energetics are also collected in ESI.†

III. Results and discussion

(1) Mechanism for the photoactivation reaction of η^5-CpCo(CO)$_2$ in the triplet state channel

We first study the photodecarbonyl reaction and the Si–H bond activation reaction of the half-sandwich two-legged-piano-stool CpCo(CO)$_2$ complex with trimethylsilane. When the CpCo(CO)$_2$ molecule absorbs light, it may jump directly from the singlet ground state to the excited states, which is called the Frank–Condon (FC) region and still has the geometry of its singlet ground state. The MP2-CAS computations are thus used in this work to compute its vertical excitation energies. As shown in the left-hand side of Fig. 2, the MP2-CAS results display eight electronic states that are achievable around the energies of a 325 nm photon: four triplet states (kcal mol^{-1}); **Co-T$_1$-FC** (42.8), **Co-T$_2$-FC** (47.1), **Co-T$_3$-FC** (69.4), and **Co-T$_4$-FC** (122.7), and four singlet states (kcal mol^{-1}); **Co-S$_1$-FC** (74.5), **Co-S$_2$-FC** (84.4), **Co-S$_3$-FC** (93.4), and **Co-S$_4$-FC** (95.5). Since the spin-allowed absorption cross-sections are well accepted to be larger than those for spin-forbidden excitations, photo-irradiation thus advances CpCo(CO)$_2$ from the singlet ground state to an excited singlet state (S_2). Then, this dicarbonyl complex relaxes to the T_1 state (**Co-T$_1$-Min**). Our calculations estimate the energy of **Co-T$_1$-Min** is about 2.6 kcal mol^{-1} above the ground-state minimum (**Co-S$_0$-Rea**). Also, we have used density functional theory to test the energy difference between the singlet and triplet η^5-CpCo(CO)$_2$ species, *i.e.*, B3PW91/Def2-TZVPPD, and B3LYP/DZP-DKH. On the basis of these

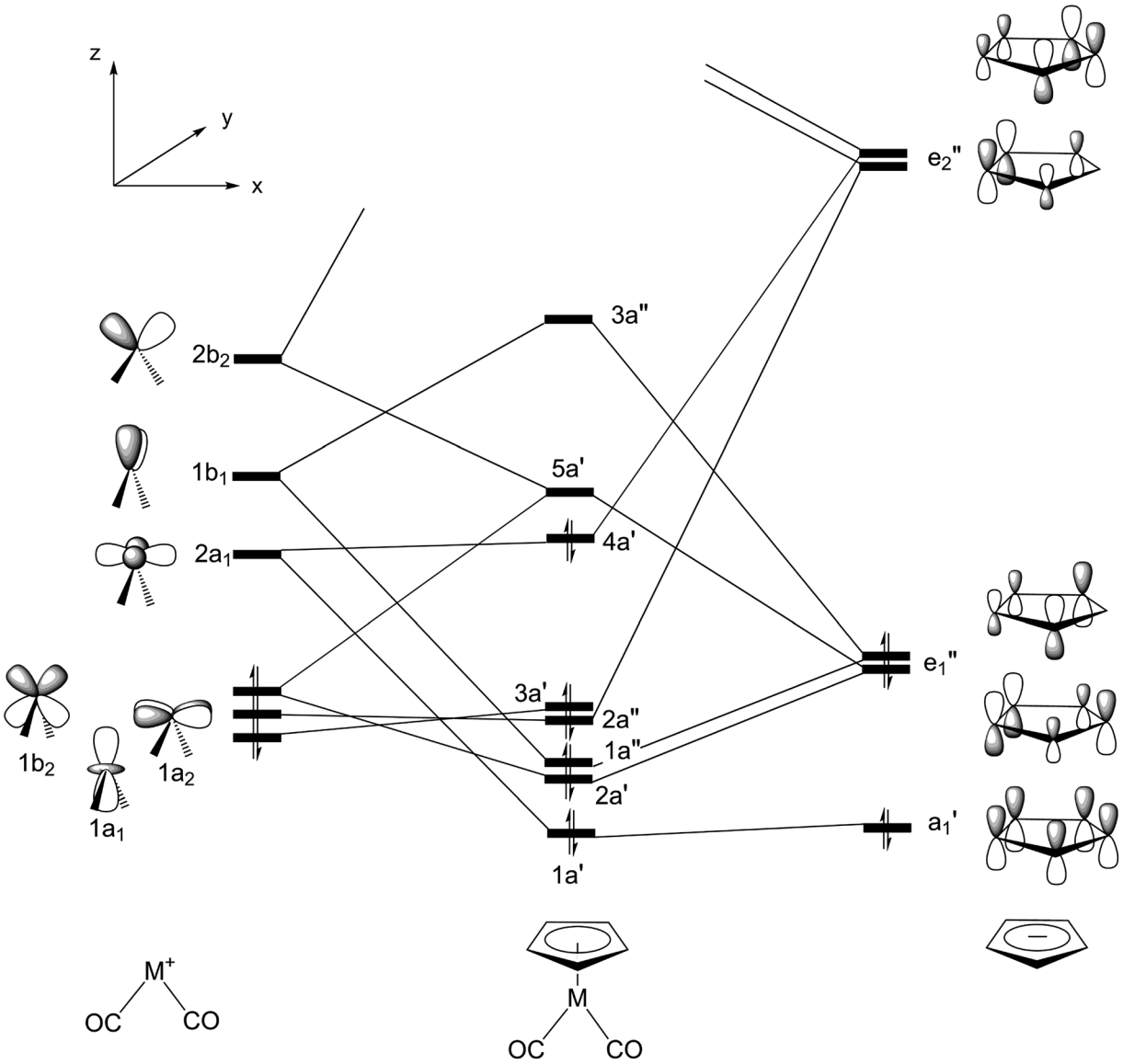

Fig. 1 Valence molecular orbitals of the group 9 η^5-CpM(CO)$_2$ (M = Co, Rh, and Ir) complex. See ref. 45–47.

computations (ESI†), the free energy of the singlet η^5-CpCo(CO)$_2$ compound is computed to be lower than that of the triplet η^5-CpCo(CO)$_2$ species by about 15 (B3PW91/Def2-TZVPPD)[66,67] and 8.6 (B3LYP/DZP-DKH)[68,69] kcal mol^{-1}, respectively.[70] Again, this reveals that its CO-photoextrusion reaction starts on the triplet state energy surface. Indeed, according to the available experiments,[24–28] it was found that excitation of this molecule at 325 nm (= 88.0 kcal mol^{-1}) leads to the generation of a η^5-CpCo(CO) intermediate in the triplet electronic state.

As seen in Fig. 2, the **Co-T_1-Min** complex then undergoes a Co–CO bond cleavage (2.066 Å) *via* a transition state (**Co-T_1-TS1**). From this transition state point, the intermediate complex may go forward three possible reaction pathways (*i.e.*, path I, path II, and path III in Fig. 2) in order to undergo an oxidative addition reaction with trimethylsilane to produce the final insertion product (**Co-S_0-Pro**).

In path I, as seen in Fig. 2, the triplet **Co-T_1-Min** molecule can dissociate one CO ligand to produce two products: one triplet CO molecule and one singlet η^5-CpCo(CO) intermediate (**Co-S_0-Int**). The relative energy of the final products ($[CO]^3$ + **Co-S_0-Int**) is, however, estimated to be 87 kcal mol^{-1} above the irradiated energy (325 nm = 88 kcal mol^{-1}).[24–28] As a result, the present computational evidence reveals that the photo-excited energy of **Co-S_0-Rea** at 325 nm is unable to generate one triplet CO and one singlet **Co-S_0-Int**. Therefore, our theoretical finding anticipates that no such photoproducts can be detected in the photochemical activation reactions for η^5-CpCo(CO)$_2$, which has been confirmed by the available experimental reports.[24–28] For convenience, the mechanism for path I of the **Co-S_0-Rea** complex can be expressed as follows:

Co system-path I: **Co-S_0-Rea** + $[Si]^1$ + $h\nu$ → **Co-T_1-FC** + $[Si]^1$ → **Co-T^1-Min** + $[Si]^1$ → **Co-T_1-TS1** + $[Si]^1$ → **Co-S_0-Int** + $[CO]^3$ + $[Si]^1$

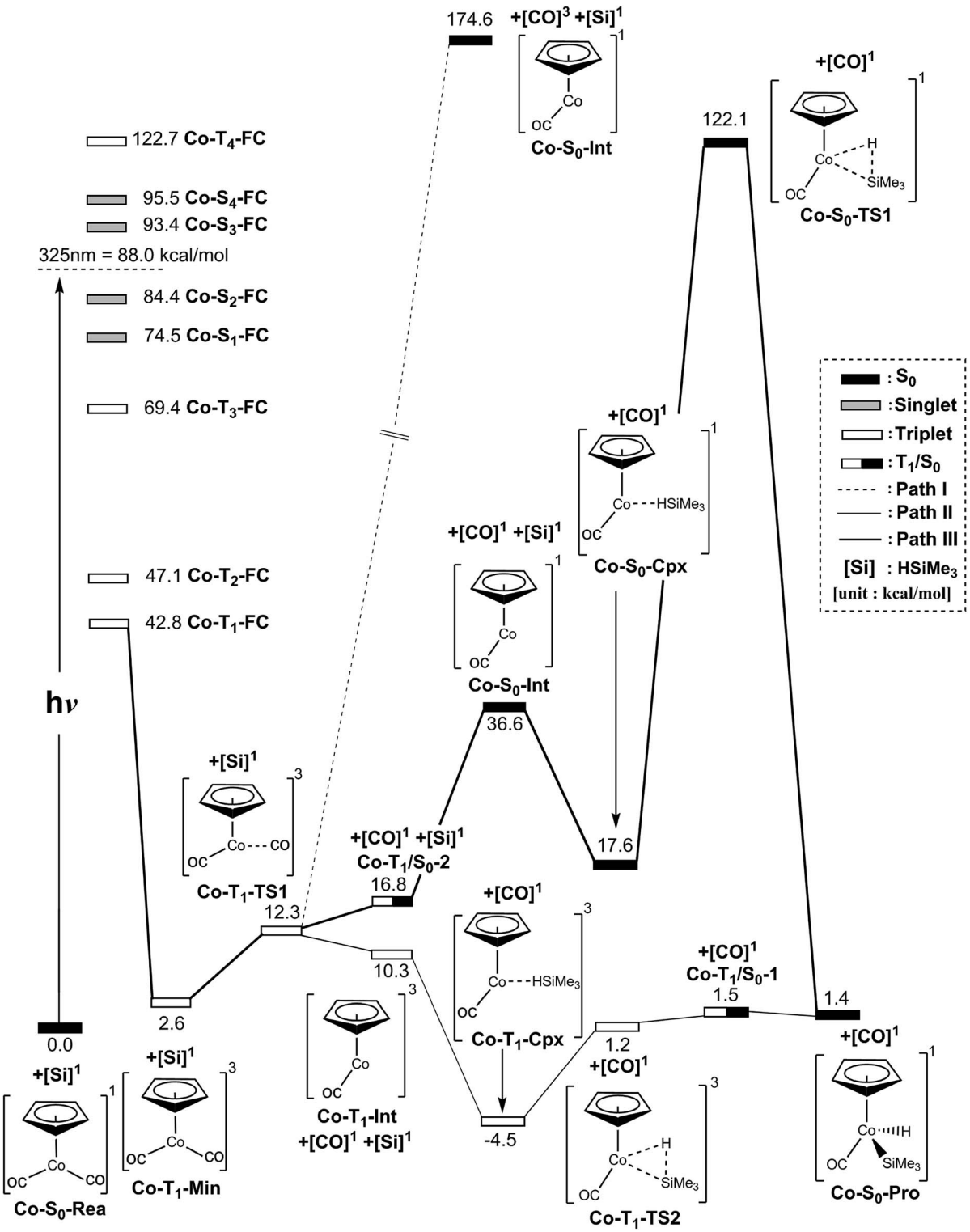

Fig. 2 Energy profiles for the photo-oxidative-addition reactions for η^5-CpCo(CO)$_2$ (**Co-S$_0$-Rea**). The computational active spaces used in this work are described in Section II. All energies (in kcal mol^{-1}) are given with respect to the reactant (**Co-S$_0$-Rea**). For the crucial points of the CASSCF optimized structures, see Fig. 3. For more information, see the text.

In the second pathway, path II, the triplet **Co-T$_1$-Min** complex can undergo one CO ligand cleavage to produce one singlet CO and one triplet **Co-T$_1$-Int** intermediate through the transition state (**Co-T$_1$-TS1**). The MP2-CAS data indicate that the **Co-T$_1$-Int** + **[CO]^1** point is computed to be about 10 kcal mol^{-1} higher than that of **Co-S$_0$-Rea**. Then, the triplet **Co-T$_1$-Int** interacts with $(CH_3)^3$Si–H to generate the precursor complex

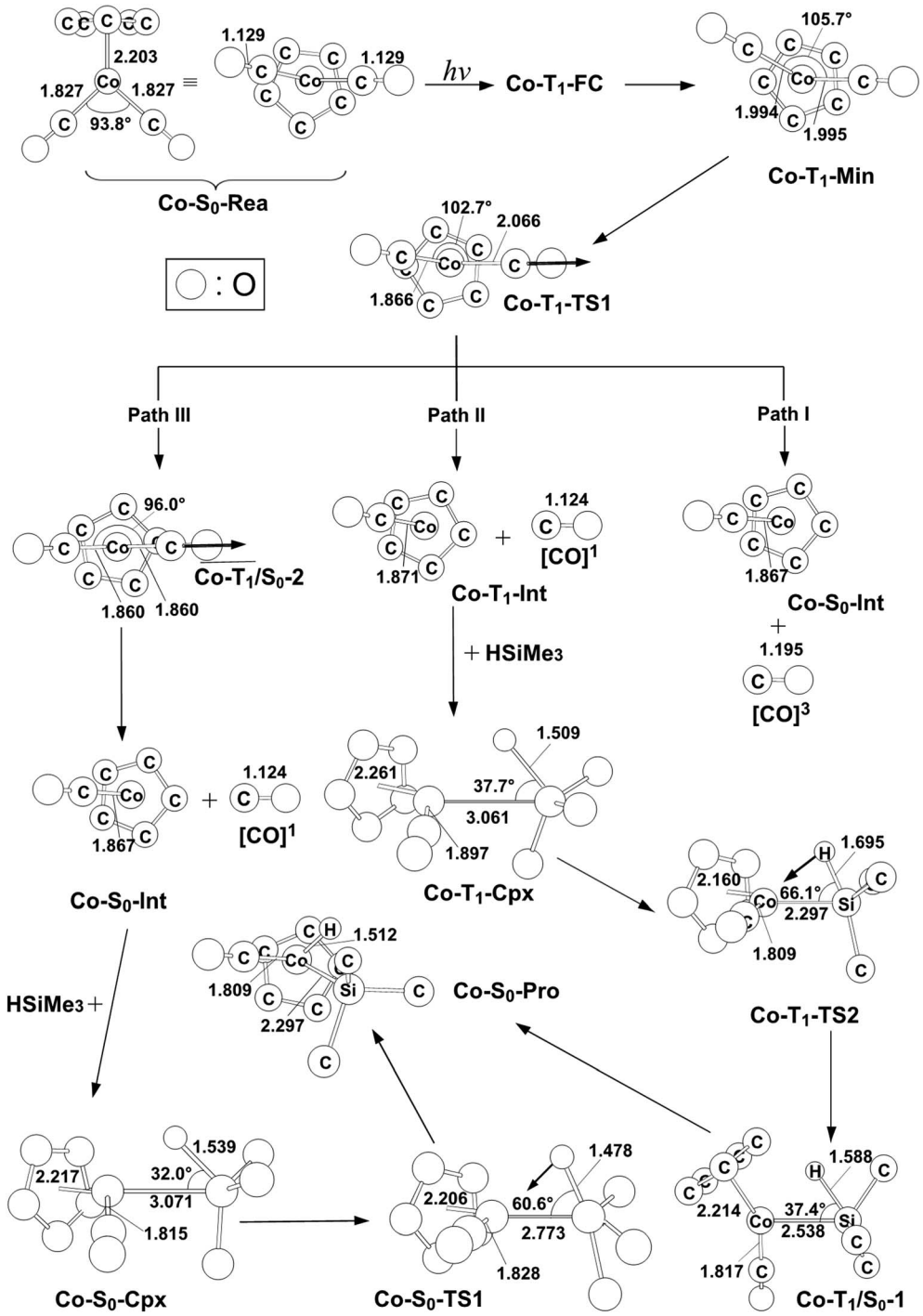

Fig. 3 The CASSCF geometries (in Å and deg) for photo-oxidative-addition reactions of η^5-CpCo(CO)$_2$ (**Co-S$_0$-Rea**). The computational active spaces used in this work are described in Section II. Their relative energies are given in Fig. 4. Some hydrogen atoms are omitted for clarity.

(**Co-T$_1$-Cpx**) in the triplet state. Subsequently, this triplet complex encounters a triplet transition state (**Co-T$_1$-TS1**) through the **Co-T$_1$/S$_0$-1** intersystem crossing to form the final singlet photoproduct (**Co-S$_0$-Pro**). On the basis of the MP2-CAS computations, path II is anticipated to be energetically accessible. The reason for this is once the initial reactants (**Co-S$_0$-Rea** + **[Si]^1**) absorb light of 325 nm (= 88 kcal mol^{-1}) wavelength, they can obtain enough energy to overcome the barrier height (5.7 kcal mol^{-1}) from **Co-T$_1$-Cpx** to **Co-T$_1$-TS2** in path II. In consequence, the mechanism for path II for both photochemical decarbonyl reaction and the Si–H bond activation reaction of η^5-CpCo(CO)$_2$ is given as follows:

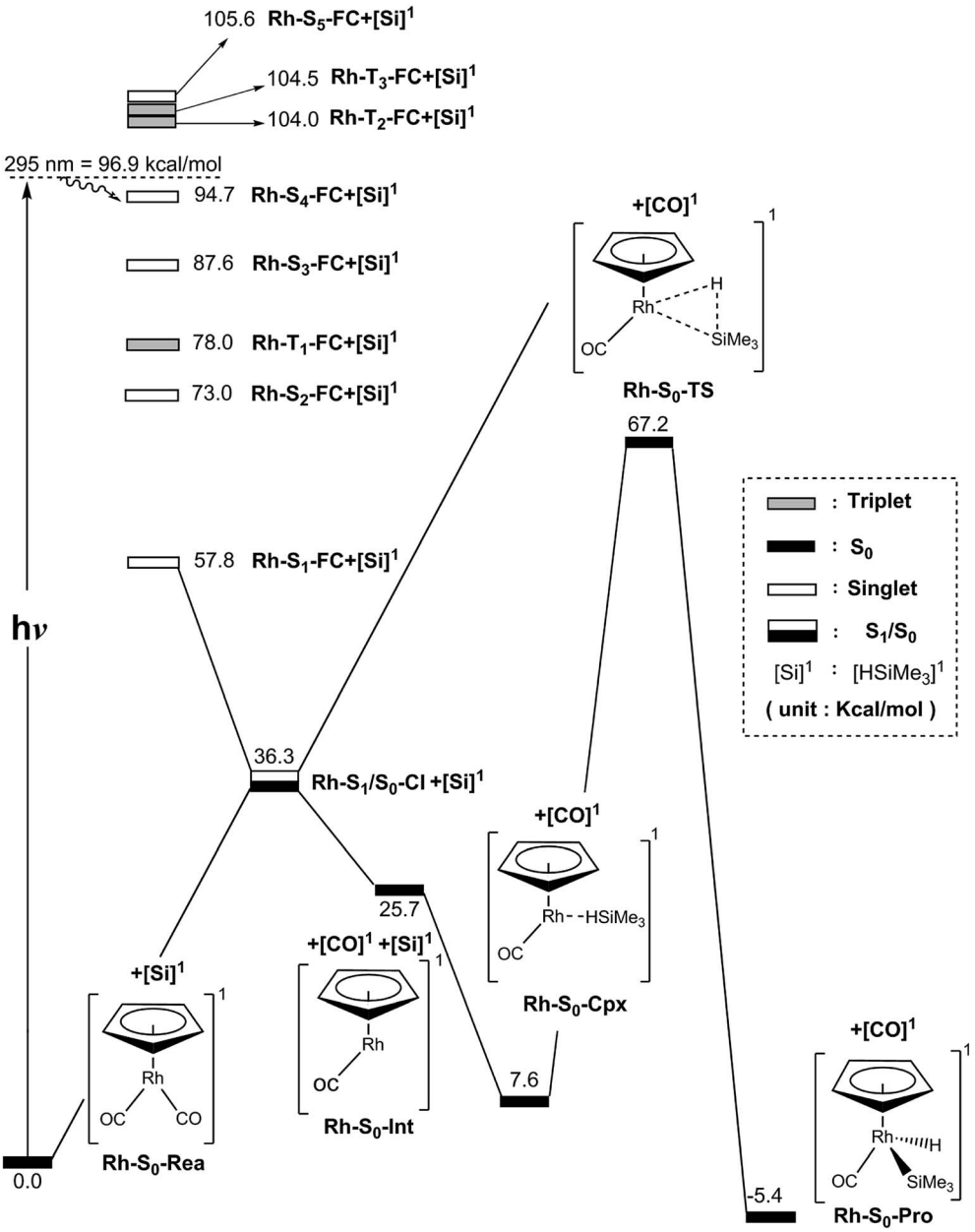

Fig. 4 Energy profiles for the photo-oxidative-addition reactions for η^5-CpRh(CO)$_2$ (**Rh-S$_0$-Rea**). The computational active spaces used in this work are described in Section II. All energies (in kcal mol^{-1}) are given with respect to the reactant (**Rh-S$_0$-Rea**). For the crucial points of the CASSCF optimized structures, see Fig. 5. For more information, see the text.

Co system-path II: **Co-S$_0$-Rea** + **[Si]^1** + $h\nu$ → **Co-T$_1$-FC** + **[Si]^1** → **Co-T$_1$-Min** + **[Si]^1** → **Co-T$_1$-TS1** + **[Si]^1** → **Co-T$_1$-Int** + **[CO]^1** + **[Si]^1** → **Co-T$_1$-Cpx** + **[CO]^1** → **Co-T$_1$-TS2** + **[CO]^1** → **Co-T$_1$/S$_0$-1** + **[CO]^1** → **Co-S$_0$-Pro** + **[CO]^1**

In path III, on the other hand, after the Co–CO bond breaking (**Co-T$_1$-TS1**), the intersystem crossing from the triplet state to the singlet state comes about in the region of the T_1/S_0 intersection (**Co-T$_1$/S$_0$-2**), as depicted in Fig. 2. By way of this crossing point, the triplet η^5-CpCo(CO)$_2$ complex separates into one singlet η^5-CpCo(CO) (**Co-S$_0$-Int**) intermediate and one singlet CO molecule. Trimethylsilane is subsequently coordinated to the central cobalt atom of the **Co-S$_0$-Int** species in the pattern of an η^2 to generate a singlet precursor complex (**Co-S$_0$-Cpx**). As a result, the Si–H bond of $(CH_3)_3Si(H)$ is broken through a singlet transition state (**Co-S$_0$-TS1**) to produce the final oxidative addition product (**Co-S$_0$-Pro**). The MP2-CAS data reveal that the energies of intermediates (**Co-S$_0$-Int** + CO + $(CH_3)_3Si(H)$), the precursor complex (**Co-S$_0$-Cpx** + CO), the transition state (**Co-S$_0$-TS1** + CO) and the final insertion product (**Co-S$_0$-Pro** + CO) relative to that of the starting materials (**Co-S$_0$-Rea** + $(CH_3)_3Si(H)$) are computed to be 37, 18, 122, and 1.4 kcal mol^{-1}, respectively. That is to say, the theoretical

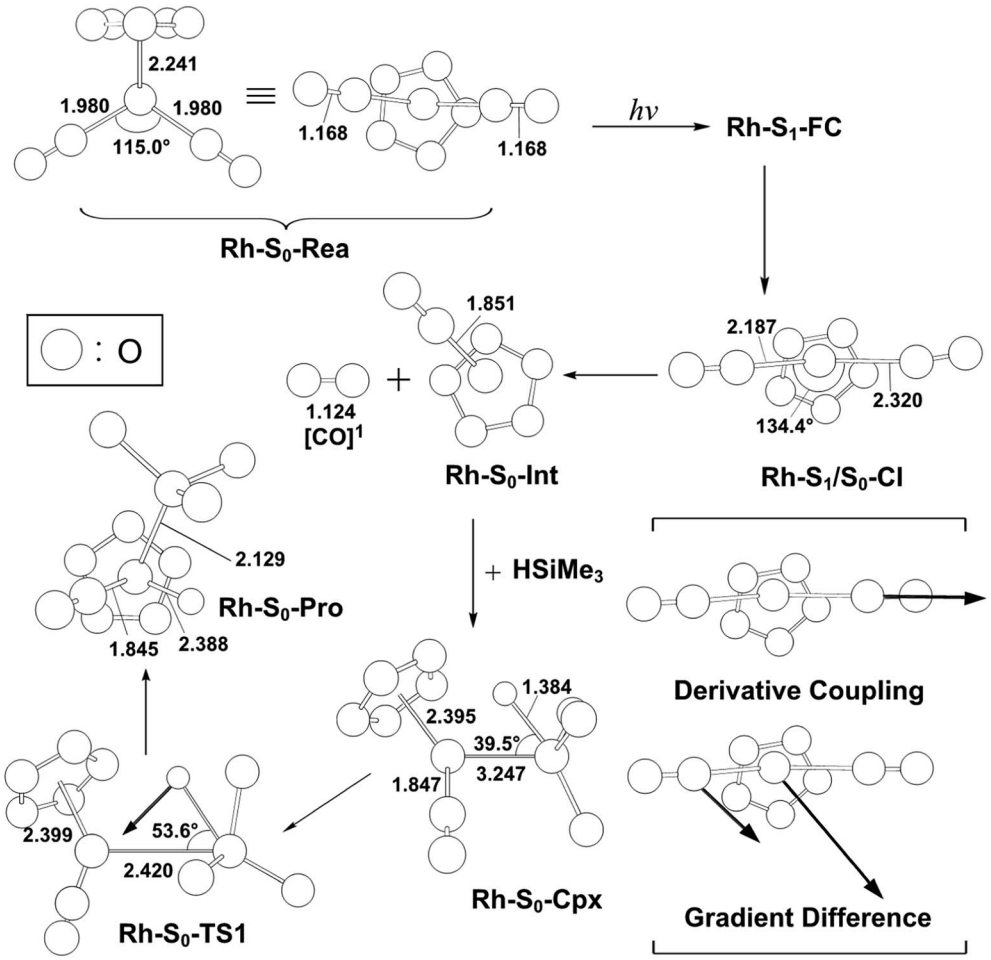

Fig. 5 The CASSCF geometries (in Å and deg) for photo-oxidative-addition reactions of η^5-CpRh(CO)$_2$ (**Rh-S$_0$-Rea**). The computational active spaces used in this work are described in Section II. Their relative energies are given in Fig. 4. Some hydrogen atoms are omitted for clarity.

calculations indicate that the energy of **Co-S$_0$-Cpx** (19 kcal mol^{-1}) is much lower than that of its further activation barrier (105 kcal mol^{-1}) from **Co-S$_0$-Cpx** to **Co-S$_0$-TS1** in path III. Our computational evidence, therefore, predicts that this singlet cobalt precursor complex (**Co-S$_0$-Cpx**) should be easily located, which has already been verified by the available experimental observations.[24–28] Furthermore, the theoretical data given in Fig. 2 show that the activation energy of **Co-S$_0$-TS1** is 105 kcal mol^{-1} much higher than the irradiation energy (325 nm = 88 kcal mol^{-1}) of the corresponding reactants (**Co-S$_0$-Rea** + $(CH_3)_3Si(H)$). That is to say, compared to the excited promotion energy, the barrier height from **Co-S$_0$-Cpx** to **Co-S$_0$-TS1** represented in path III cannot be surmounted. Accordingly, path III is energetically unfavorable for such photochemical oxidative additions of the η^5-CpCo(CO)$_2$ compound. Thus, the present theoretical investigations suggest that the mechanism of path III should proceed as follows:

Co system-path III: **Co-S$_0$-Rea** + **[Si]^1** + *hν* → **Co-T$_1$-FC** + **[Si]^1** → **Co-T$_1$-Min** + **[Si]^1** → **Co-T$_1$-TS1** + **[Si]^1** → **Co-T$_1$/S$_0$-2** + **[CO]^1** + **[Si]^1** → **Co-S$_0$-Int** + **[CO]^1** + **[Si]^1** → **Co-S$_0$-Cpx** + **[CO]^1** → **Co-S$_0$-TS1** + **[CO]^1** → **Co-S$_0$-Pro** + **[CO]^1**

In brief, the above computations reveal that once the η^5-CpCo(CO)$_2$ (**Co-S$_0$-Rea**) molecule absorbs light, it can easily generate a coordinatively unsaturated 16-electron η^5-CpCo(CO) fragment in either the triplet or the singlet excited state, *via* the loss of a CO molecule upon photolysis. In a similar way, this dynamic half-sandwich intermediate can easily undergo oxidative addition to the Si–H bond of H–Si(Me)$_3$. Three reaction routes (paths I, II, and III) can be used for interpreting the mechanisms of such CO-photoextrusion reaction as well as the Si–H bond activation reaction. The present theoretical evidence demonstrate that only path II, which can form the triplet **Co-T$_1$-Int** fragment, is the most energetically favorable reaction path for the photochemical reactions. On the other hand, both path I and path III, which can produce the singlet **Co-S$_0$-Int** species, are energetically unfeasible for the generation of **Co-S$_0$-Pro**. In other words, our theoretical investigations strongly indicate that it is only the triplet species, $[\eta^5$-CpCo(CO)$]^3$ (**Co-T$_1$-Int**), that play a decisive role in the photochemical Si–H bond activation reaction by the organometallic compound, η^5-CpCo(CO)$_2$. These theoretical findings are in excellent agreement with the experimental observations reported by the team led by Harris.[24–28]

(2) Mechanism for the photoactivation reaction of η^5-CpRh(CO)$_2$ in the singlet state channel

For comparison with the case of η^5-CpCo(CO)$_2$, we next examine the mechanism of the photoactivation reaction of η^5-CpRh(CO)$_2$ (**Rh-S$_0$-Rea**) towards trimethylsilane. The same theoretical method (MP2-CAS) is utilized to explore the potential energy surfaces of **Rh-S$_0$-Rea** for its Si–H bond activation reactions, which are all shown in Fig. 4. The selected geometrical parameters for the photochemical activation reaction of **Rh-S$_0$-Rea** with trimethylsilane are given in Fig. 5. According to some availably experimental observations,[23,29,30] Harris and coworkers reported that the irradiation of light to **Rh-S$_0$-Rea** is 295 nm (= 96.9 kcal mol^{-1}).

As seen in the left-hand side of Fig. 4, the MP2-CAS computational data indicates that the relative FC energies (kcal mol^{-1}) of the electronic states increase in the order: **Rh-S$_1$-FC** (57.8) < **Rh-S$_2$-FC** (73.0) < **Rh-T$_1$-FC** (78.0) < **Rh-S$_3$-FC** (87.6) < **Rh-S$_4$-FC** (94.7) < **Rh-T$_2$-FC** (104.0) < **Rh-T$_3$-FC** (104.5) < **Rh-S$_5$-FC** (105.6). The MP2-CAS results reveal that only the energy of the first excited triplet state (*i.e.*, **Rh-T$_1$-FC**) is lower than that of its photoirradiated light (295 nm). In addition, we did not calculate the triplet energy surface for the photodecarbonyl reaction of the η^5-CpRh(CO)$_2$ (**Rh-S$_0$-Rea**) complex in the present work. First, on the basis of the available experimental results,[23,29,30] the photolysis of η^5-CpRh(CO)$_2$ generates only one singlet η^5-CpRh(CO) fragment and one singlet CO molecule, *i.e.*, $[\eta^5\text{-CpRh(CO)}_2]^1 + h\nu \rightarrow [\eta^5\text{-CpRh(CO)}]^1 + \mathbf{[CO]^1}$. Second, it is well understood that spin-allowed (*e.g.*, singlet ground state → singlet excited state) absorption cross-sections are basically larger than those for spin-forbidden excitations (*e.g.* singlet ground state → triplet excited state). Due to the above two reasons, photoexcitation can promote the η^5-CpRh(CO)$_2$ complex from a singlet ground state a singlet excited state (such as, S_4 or S_3 in Fig. 4). Then, this excited complex relaxes to its singlet ground state. As a consequence, we focus the on the singlet state surface of the photodecarbonyl reaction of η^5-CpRh(CO)$_2$ from now on.

It has to be mentioned here that this work starting on the singlet surface of η^5-CpRh(CO)$_2$ does not imply its triplet excited states do not play a role in such a photochemical CO-extrusion reaction. In contrast, we understand the complexity of the photochemical behaviors of the η^5-CpRh(CO)$_2$ complex. In order to make the present study simpler and clear, we thus consider the singlet energy surface aspects separately. The photochemical behavior of the triplet excited state is considered later as an effect, which may or may not affect the photochemistry of the η^5-CpRh(CO)$_2$ complex.

On the basis of the above information, our computations therefore suggest that once the **Rh-S$_0$-Rea** complex has absorbed the light, it will jump from the singlet ground state to the more highly excited singlet state (**Rh-S$_4$-FC**) and then relaxes to the lowest excited singlet state (**Rh-S$_1$-FC**). Accordingly, in this work we use the conical intersection (CI) concept,[57–67] which considers the crossing between states of the same multiplicity (mostly commonly singlet–singlet), to explore the mechanism of the photochemical activation reactions of the **Rh-S$_0$-Rea** system.

As shown in Fig. 4, after the vertical excitation procedure, the **Rh-S$_0$-Rea** complex finally decays to the excited singlet **Rh-S$_1$-FC** point but still maintains the ground-state geometry. Subsequently, this species relaxes to arrive at a **Rh-S$_1$/S$_0$-CI** point, from which the photoexcited rhodium complex decays non-radiatively to the singlet ground state.[57–67] Our MP2-CAS findings suggest that **Rh-S$_1$/S$_0$-CI** is about 22 kcal mol^{-1} lower in energy than **Rh-S$_1$-FC**. In Fig. 4, the directions of the derivative coupling and gradient difference vectors for the **Rh-S$_1$/S$_0$-CI** point are given. That is to say, funneling through **Rh-S$_1$/S$_0$-CI** *via* either the gradient difference vector or the derivative coupling vector can result in two different reaction routes on the singlet ground state surface. As shown in Fig. 4, the major contribution of the derivative coupling vector concerns the Rh–CO bond breaking, whereas the gradient difference vector involves vibrationally hot motion at the ground state configuration. As a result, the former allows the formation of the coordinatively unsaturated 16-electron η^5-CpRh(CO) (**Rh-S$_0$-Int**) intermediate and one CO molecule, both of which are in the singlet ground states. Indeed, this finding has been confirmed by the experimental observations, in which the photodecarbonyl reaction of **Rh-S$_0$-Rea** finally occurs a singlet 16-electron organometallic η^5-CpRh(CO) species.[23,29,30]

Subsequently, **Rh-S$_0$-Int** interacts with Si(H)Me$_3$ to form a singlet precursor complex (**Rh-S$_0$-Cpx**), whose energy is

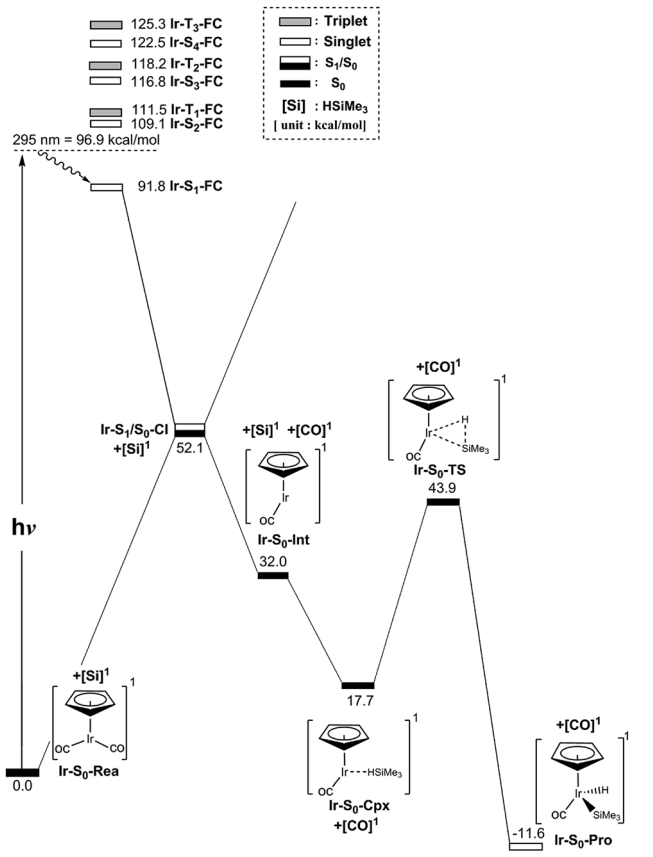

Fig. 6 Energy profiles for the photo-oxidative-addition reactions for η^5-CpIr(CO)$_2$ (**Ir-S$_0$-Rea**). The computational active spaces used in this work are described in Section II. All energies (in kcal mol^{-1}) are given with respect to the reactant (**Ir-S$_0$-Rea**). For the crucial points of the CASSCF optimized structures, see Fig. 7. For more information, see the text.

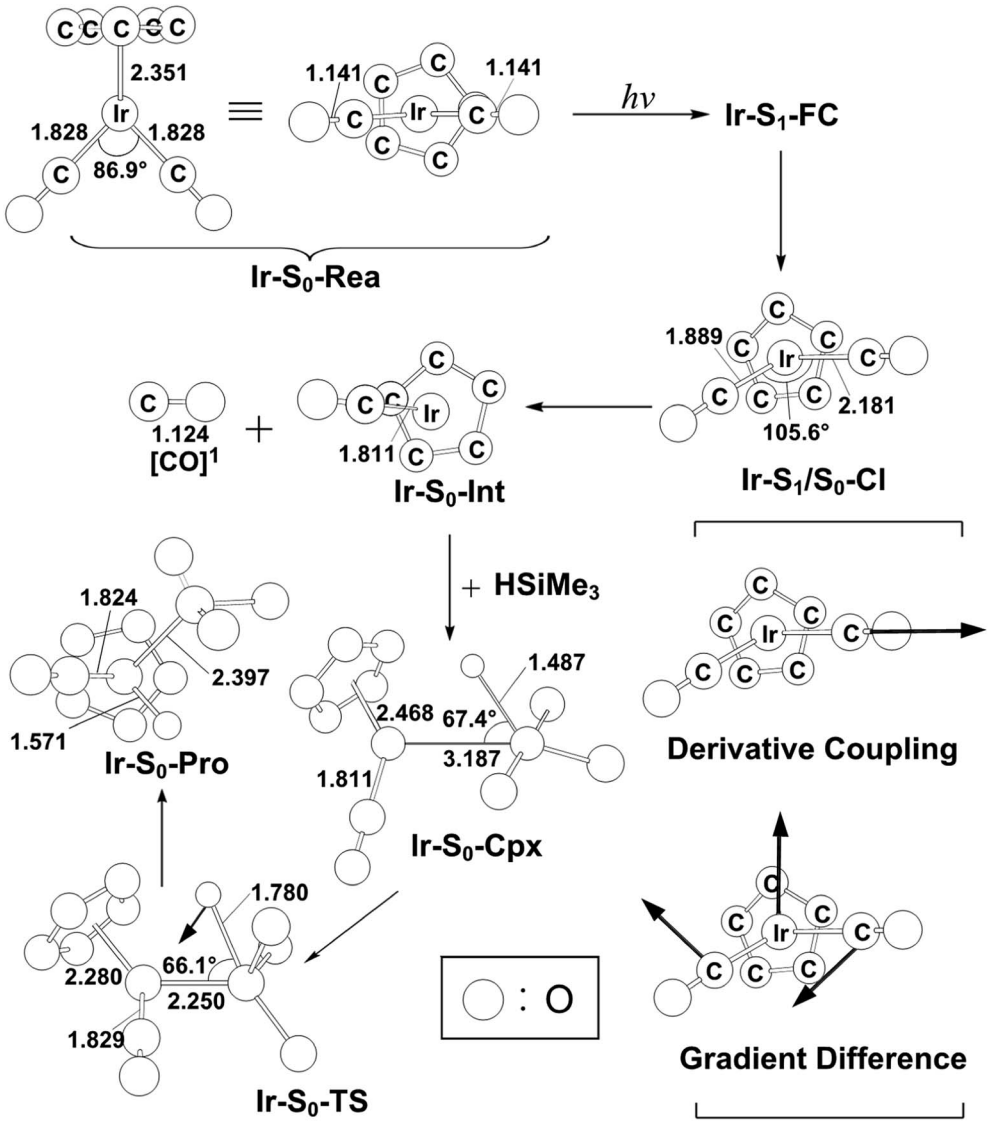

Fig. 7 The CASSCF geometries (in Å and deg) for photo-oxidative-addition reactions of η^5-CpIr(CO)$_2$ (**Ir-S$_0$-Rea**). The computational active spaces used in this work are described in Section II. Their relative energies are given in Fig. 6. Some hydrogen atoms are omitted for clarity.

predicted to be 7.6 kcal mol^{-1} above the energy of the corresponding reactants (**Rh-S$_0$-Rea** + $(CH_3)_3Si(H)$). Then, **Rh-S$_0$-Cpx** undergoes the oxidative addition into the Si–H bond of trimethylsilane *via* the transition state, **Rh-S$_0$-TS**. Our computational findings suggest that the relative energies (kcal mol^{-1}) of **Rh-S$_0$-Cpx**, **Rh-S$_0$-TS** and **Rh-S$_0$-Pro** with respect to the corresponding reactants are 7.6, 67.2, and −5.4, respectively. As a result, from the reaction profiles given in Fig. 4, it is clear that the photoexcitation energy at 295 nm of the η^5-CpRh(CO)$_2$ reactant has sufficient internal energy to overcome the energy barrier from **Rh-S$_0$-Cpx** to **Rh-S$_0$-TS**. In brief, the theoretical observations demonstrate that the conical intersection mechanism plays a decisive role in the mechanism of the Si–H bond-activation reaction of photogenerated singlet η^5-CpRh(CO) with trimethylsilane. Therefore, the mechanism of singlet photochemical oxidative addition reaction of η^5-CpRh(CO)$_2$ can be represented as follows:

Rh system: **Rh-S$_0$-Rea** + **[Si]^1** + $h\nu$ → **Rh-S$_1$-FC** + **[Si]^1** → **Rh-S$_1$/S$_0$-CI** + **[Si]^1** → **Rh-S$_0$-Int** + **[CO]^1** + **[Si]^1** → **Rh-S$_0$-Cpx** + **[CO]^1** → **Rh-S$_0$-TS** + **[CO]^1** → **Rh-S$_0$-Pro** + **[CO]^1**

3(3) Mechanism for the photoactivation reaction of η^5-CpIr(CO)$_2$ in the singlet state channel

In spite of the fact that the photochemical behavior of η^5-CpIr(CO)$_2$ (**Ir-S$_0$-Rea**) has been experimentally reported elsewhere, unlike its cobalt and rhodium counterparts,[24–29] the photodecarbonyl mechanism of **Ir-S$_0$-Rea** has not been investigated neither experimentally nor theoretically.[30–34]

In this work, the same computational method (MP2-CAS) is used to theoretically investigate the potential energy surfaces of η^5-CpIr(CO)$_2$ for its photochemical oxidative reaction. The computational reaction routes and the related geometrical

parameters for the photoactivation reaction of **Ir-S_0-Rea** with trimethylsilane are schematically represented in Fig. 6 and 7, respectively. To enable comparisons with the previous η^5-CpCo(CO)$_2$ (**Co-S_0-Rea**) and η^5-CpRh(CO)$_2$ (**Rh-S_0-Rea**) model systems, the irradiation of light to **Ir-S_0-Rea** is assumed to be 295 nm (= 96.9 kcal mol^{-1}), as shown on the left-hand side of Fig. 6.

On the basis of the MP2-CAS computational data, Fig. 6 demonstrates that the lowest vertically excited energy state in the FC region is **Ir-S_1-FC** (91.8 kcal mol^{-1}), whose energy is notably lower than that of its irradiation of light (96.9 kcal mol^{-1}). That is to say, the present theoretical observations indicate that the half-sandwich reactant complex (**Ir-S_0-Rea**) is initially irradiated to its lowest lying singlet excited state (**Ir-S_1-FC**). In the current work, we thus concentrate below on the singlet state channel for the photochemical activation reaction of **Ir-S_0-Rea** with Si(CH$_3$)$_3$(H) from now on.

Subsequently, from the **Ir-S_1-FC** point, this excited species relaxes to the conical intersection point (**Ir-S_1/S_0-CI**), whose energy is calculated to be about 52 kcal mol^{-1} relative to that of its corresponding reactant. Funneling through the **Ir-S_1/S_0-CI** point, several reaction routes on the ground-state energy surface may be foreseen by following its derivative coupling and the gradient difference vectors, which are already collected in Fig. 7. It is apparent from Fig. 7 that the main contribution of the gradient difference vector is the bending motions of two C–O bonds that result in a vibrationally hot **Ir-S_0-Rea** molecule, whereas the derivative coupling vector corresponds to an Ir–CO bond cleavage. Therefore, following the derivative coupling vector from **Ir-S_1/S_0-CI** (Fig. 7) can give rise to the generation of one singlet CO molecule and one singlet half-sandwich monocarbonyl η^5-CpIr(CO) intermediate (**Ir-S_0-Int**). The MP2-CAS computations, which are given in Fig. 6, reveal that this **Ir-S_0-Int** + CO + Si(CH$_3$)$_3$(H) point is 32.0 kcal mol^{-1} above the corresponding singlet reactants. Then the **Ir-S_0-Int** species interacts with Si(CH$_3$)$_3$(H) to yield a precursor complex, **Ir-S_0-Cpx**, whose energy is estimated to be about 18 kcal mol^{-1} with respect to the corresponding singlet state species. Finally, this activated complex undergoes its oxidative addition reaction *via* a transition state (**Ir-S_0-TS**) to lead to the formation of a photoproduct, **Ir-S_0-Pro**, as demonstrated in Fig. 6. Our MP2-CAS data indicate that the energy barrier from **Ir-S_0-Cpx** to **Ir-S_0-TS** and the reaction enthalpy of **Ir-S_0-Pro** are estimated to be about 26 and −12 kcal mol^{-1}, respectively. From the reaction profile given in Fig. 6, it is clear that the **Ir-S_0-Rea** molecule has sufficient internal energy (38 kcal mol^{-1}) to overcome the energy barrier between **Ir-S_0-Cpx** and **Ir-S_0-TS** (26 kcal mol^{-1}) to reach the final insertion product (**Ir-S_0-Pro**), after the photoexcited **Ir-S_0-Rea** relaxes to the CI point (**Ir-S_1/S_0-CI**). Accordingly, the mechanism of the photoactivation reaction of η^5-CpIr(CO)$_2$ with trimethylsilane can be described as follows: **[Si]^1** stands for Si(CH$_3$)$_3$(H) at the singlet state.

Ir system: **Ir-S_0-Rea** + **[Si]^1** + $h\nu$ → **Ir-S_1-FC** + **[Si]^1** → **Ir-S_1/S_0-CI** + **[Si]^1** → **Ir-S_0-Int** + **[CO]^1** + **[Si]^1** → **Ir-S_0-Cpx** + **[CO]^1** → **Ir-S_0-TS** + **[CO]^1** → **Ir-S_0-Pro** + **[CO]^1**

IV. Conclusion

The photochemical Si–H bond activation reactions by the group 9, d^8 organometallic molecules, η^5-CpM(CO)$_2$ (M = Co, Rh, and Ir), have been studied by using the CAS as well as MP2-CAS computational methods. Taking all the model conclusions obtained in this work together yield the following summary:

(1) Our model computations demonstrate that upon absorption of a photon of light, η^5-CpCo(CO)$_2$ (**Co-S_0-Rea**) is promoted vertically to one higher excited state and then relaxes to the triplet FC point, **Co-T_1-FC**. From this point, this cobalt complex returns to the triplet minimum species, **Co-T_1-Min**. After its photochemical decarbonylation, three important reaction pathways (paths I, II, and III) have been considered to examine its oxidative addition of a Si–H bond with Si(H)Me$_3$. The theoretical observations indicate that **Co-S_0-Rea** initiates from the excited triplet state surface and finally changes to the singlet ground-state pathway. In other words, the intersystem crossing between the triplet (T_1) and singlet (S_0) surfaces must play a vital role in describing the mechanisms for the photochemical CO-extrusion and oxidative addition reactions of the **Co-S_0-Rea** complex. Our theoretical findings strongly suggest that path II is the most energetically favorable reaction route for such alkylsilane activation reactions. In particular, the computational examinations reveal that the triplet monocarbonyl species ([η^5-CpCo(CO)]^3) plays a dominant role, but the corresponding singlet intermediate ([η^5-CpCo(CO)]^1) plays no role, in the photochemical CO-extrusion reaction and its subsequent activation reaction for a Si–H bond in alkylsilane. The above theoretical conclusions have previously been verified by some experimental findings.[24–36]

(2) On the other hand, after the CO-photoextrusions of η^5-CpRh(CO)$_2$ (**Rh-S_0-Rea**) and η^5-CpIr(CO)$_2$ (**Ir-S_0-Rea**), our theoretical findings demonstrate that their half-sandwich monocarbonyl intermediates (**Rh-S_0-Int** and **Ir-S_0-Int**) should still proceed on the singlet energy surfaces. In other words, the conical intersection plays a central role in determining the mechanisms of their photochemical oxidative addition reactions with alkylsilanes.

Conflicts of interest

There are no conflicts to declare.

Acknowledgements

The authors are grateful to the National Center for High-Performance Computing of Taiwan for generous amounts of computing time, and the Ministry of Science and Technology of Taiwan for the financial support. One of the author (Ming-Der Su) also wishes to thank Professor Michael A. Robb, Dr Michael J. Bearpark, Dr S. Wilsey, (University of London, UK) and Professor Massimo Olivucci (Universita degli Studi di Siena, Italy) for their encouragement and support during his stay in London. Special thanks are also due to reviewers 1 and 2 for very helpful suggestions and comments.

References

1 P. P. Deutsch and R. Eisenberg, Stereochemistry of Hydrogen Oxidative Addition and Dihydride-Transfer Reactions Involving Iridium(I) Complexes, *Chem. Rev.*, 1988, **88**, 1147–1161.

2 L. M. Rendina and R. J. Puddephatt, Oxidative Addition Reactions of Organoplatinum(II) Complexes with Nitrogen-Donor Ligands, *Chem. Rev.*, 1997, **97**, 1735–1754.

3 G. Zeni and R. C. Larock, Synthesis of Heterocycles *via* Palladium-Catalyzed Oxidative Addition, *Chem. Rev.*, 2006, **106**, 4644–4680.

4 L. Souillart and N. Cramer, Catalytic C–C Bond Activations *via* Oxidative Addition to Transition Metals, *Chem. Rev.*, 2015, **115**, 9410–9464.

5 R. H. Crabtree, Dihydrogen Complexation, *Chem. Rev.*, 2016, **116**, 8750–8769.

6 J. Y. Corey, Reactions of Hydrosilanes with Transition Metal Complexes, *Chem. Rev.*, 2016, **116**, 11291–11435.

7 H. G. Schuster-Woldan and F. Basolo, Kinetics and Mechanism of Substitution Reactions of π-Cyclopentadienyldicarbonylrhodium, *J. Am. Chem. Soc.*, 1966, **88**, 1657–1663.

8 W. P. Weiner, M. A. White and R. G. Bergman, Direct Observation of Alkyl/Nitrosyl Migratory Insertion in an Organotransition Metal Complex, *J. Am. Chem. Soc.*, 1981, **103**, 3612–3614.

9 A. H. Janowicz, J. H. Bryndza and R. G. Bergman, Phosphine Substitution in (η^5-cyclopentadienyl) bis(triphenylphosphine)cobalt(I): Evidence for a Dissociative Mechanism, *J. Am. Chem. Soc.*, 1981, **103**, 1516–1518.

10 A. H. Janowicz and R. G. Bergman, Carbon-Hydrogen Activation in Completely Saturated Hydrocarbons: Direct Observation of M + R-H → M(R)(H), *J. Am. Chem. Soc.*, 1982, **104**, 352–354.

11 J. K. Hoyano and W. A. G. Graham, Oxidative Addition of the Carbon-Hydrogen Bonds of Neopentane and Cyclohexane to a Photochemically Generated Iridium(I) Complex, *J. Am. Chem. Soc.*, 1982, **104**, 3723–3725.

12 W. D. Jones and F. J. Feher, Mechanism of arene carbon-hydrogen bond activation by $(C_5Me_5)Rh(PMe_3)(H)Ph$. Evidence for arene precoordination, *J. Am. Chem. Soc.*, 1982, **104**, 4240–4242.

13 E. P. Wasserman, R. G. Bergman and C. B. Moore, IR Flash Kinetic Spectroscopy of Transients Generated by Irradiation of $(\eta^5\text{-}C_5H_5)Co(CO)_2$ in the Gas Phase and in Solution, *J. Am. Chem. Soc.*, 1988, **110**, 6076–6084.

14 A. H. Janowicz and R. G. Bergman, Activation of Carbon-Hydrogen Bonds in Saturated Hydrocarbons on Photolysis of $(\eta^5\text{-}C_5Me_5)(PMe_3)IrH_2$. Relative Rates of Reaction of the Intermediate with Different Types of Carbon-Hydrogen Bonds and Functionalization of the Metal-Bound Alkyl Groups, *J. Am. Chem. Soc.*, 1983, **105**, 3929–3939.

15 J. K. Hoyano, A. D. McMaster and W. A. G. Graham, Activation of Methane by Iridium Complexes, *J. Am. Chem. Soc.*, 1983, **105**, 7190–7191.

16 B. H. Weiller, E. P. Wasserman, R. G. Bergman, C. B. Moore and G. C. Pimentelt, Time-resolved IR Spectroscopy in Liquid Rare Gases: Direct Rate Measurement of an Intermolecular Alkane Carbon-Hydrogen Oxidative Addition Reaction, *J. Am. Chem. Soc.*, 1989, **111**, 8288–8290.

17 T. P. Dougherty and E. J. Heilweil, Transient Infrared Spectroscopy of $(\eta^5\text{–}C_5\ H_5)Co(CO)_2$ Photoproduct Reactions in Hydrocarbon Solutions, *J. Chem. Phys.*, 1994, **100**, 4006–4009.

18 A. A. Bengali, R. G. Bergman and C. B. Moore, Evidence for the Formation of Free 16-Electron Species Rather than Solvate Complexes in the Ultraviolet Irradiation of $CpCo(CO)_2$ in Liquefied Noble Gas Solvents, *J. Am. Chem. Soc.*, 1995, **117**, 3879–3880.

19 A. J. Rest, I. Whitwell, W. A. G. Graham, J. K. Hoyano and A. D. McMaster, Photoactivation of Methane by η^5-Cyclopentadienyl and Substituted η^5-Cyclopentadienyl Group 8 Metal Dicarbonyl Complexes, $[M(\eta^5\text{-}C_5R_5)(CO)_2]$ (M = Rh or Ir, R = H or Me), and Dicarbonyl(η^5-indenyl) iridium: A Matrix Isolation Study, *J. Chem. Soc., Dalton Trans.*, 1987, **16**, 1181–1190.

20 E. P. Wasserman, C. B. Moore and R. G. Bergman, Gas-Phase Rates of Alkane C–H Oxidative Addition to a Transient CpRh(CO) Complex, *Science*, 1992, **255**, 315–318.

21 W.-S. Lee and H. Brintzinger, Reactive Intermediates in the Photolysis of cyclopentadienylcobalt(I) Dicarbonyl and in the Reduction of Cyclopentadienylcobalt (III) Carbonyl Diiodide, *J. Organomet. Chem.*, 1977, **127**, 87–92.

22 W. Jetz and W. A. G. Graham, Silicon-transition Metal Chemistry. I. Photochemical Preparation of Silyl(transition metal) Hydrides, *Inorg. Chem.*, 1971, **10**, 4–9.

23 S. T. Belt, F. W. Grevels, W. E. Klotzbuecher, A. McCamley and R. N. Perutz, Intermediates in the Time-resolved and Matrix Photochemistry of (η^5-Cyclopentadienyl)rhodium Complexes. Roles of Alkane Activation and Rhodium-Rhodium Bond Formation, *J. Am. Chem. Soc.*, 1989, **111**, 8373–8382.

24 K. T. Kotz, H. Yang, P. T. Snee, C. K. Payne and C. B. Harris, Organometallic Complexes for Nonlinear Optics: Part 19. Syntheses and Molecular Quadratic Hyperpolarizabilities of Indoanilino–alkynyl–ruthenium Complexes, *J. Organomet. Chem.*, 2000, **596**, 183–192.

25 P. T. Snee, C. K. Payne, K. T. Kotz, H. Yang and C. B. Harris, Triplet Organometallic Reactivity under Ambient Conditions: An Ultrafast UV Pump/IR Probe Study, *J. Am. Chem. Soc.*, 2001, **123**, 2255–2264.

26 H. Yang, K. T. Kotz, M. C. Asplund, M. J. Wilkens and C. B. Harris, Ultrafast Infrared Studies of Bond Activation in Organometallic Complexes, *Acc. Chem. Res.*, 1999, **32**, 551–560.

27 J. P. Lomont, S. C. Nguyen, J. P. Schlegel, M. C. Zoerb, A. D. Hill and C. B. Harris, Ultrafast Observation of a Solvent Dependent Spin State Equilibrium in CpCo(CO), *J. Am. Chem. Soc.*, 2012, **134**, 3120–3126.

28 B. Sztáray and T. Baer, Dissociation Dynamics and Thermochemistry of Energy-Selected $CpCo(CO)_2^+$ Ions, *J. Am. Chem. Soc.*, 2000, **122**, 9219–9226.

29 D. P. Drolet and A. J. Lees, Photochemistry of (η^5-C_5H_5)$Rh(CO)_2$ in Phosphine Solutions: Evidence for an Associative Photosubstitution Mechanism, *J. Am. Chem. Soc.*, 1990, **112**, 5878–5879.

30 Z. Hu, R. J. Boyd and H. Nakatsuji, Molecular structures and Excited States of $CpM(CO)_2$ (Cp = η^5-C5H5); M = Rh, Ir) and $[Cl_2Rh(CO)_2]^-$. Theoretical Evidence for a Competitive Charge Transfer Mechanism, *J. Am. Chem. Soc.*, 2002, **124**, 2664–2671.

31 X. Li, G. M. Bancroft, R. J. Puddephatt, Y.-F. Hu and K. H. Tan, Variable-Energy Photoelectron Spectroscopy of $CpM(CO)_2$ (M = Co, Rh, Ir): Molecular Orbital Assignments and an Evaluation of the Difference in Ground-State Orbital Characters, *Organometallics*, 1996, **15**, 2890–2904.

32 J. A. Banister, A. I. Cooper, S. M. Howdle, M. Jobling and M. Poliakoff, Solvent-Free" Photochemical Activation of CH_4, C_2H_4, and C_2H_6 by (C_5Me_5)$Ir(CO)_2$ in Supercritical Fluid Solution, *Organometallics*, 1996, **15**, 1804–1812.

33 K. H. G. Mak, P. K. Chan, W. Y. Fan, R. Ganguly and W. K. Leong, Photochemical Reaction of $Cp^*Ir(CO)_2$ with C6F5X (X = CN, F): Formation of Diiridium(II) Complexes, *Organometallics*, 2013, **32**, 1053–1059.

34 P. K. Chan and W. K. Leong, Reaction of $Cp^*Ir(CO)_2$ with Activated Perfluoroaromatic Compounds: Formation of Metallocarboxylic Acids *via* Aromatic Nucleophilic Substitution, *Organometallics*, 2007, **27**, 1247–1253.

35 T. Ziegler, V. Tschinke, L. Fan and A. D. Becke, Theoretical Study on the Electronic and Molecular Structures of (C_5H_5)M(L) (M = Rhodium, Iridium; L = Carbonyl, Phosphine) and $M(CO)_4$ (M = Ruthenium, Osmium) and Their Ability to Activate the Carbon-Hydrogen Bond in Methane, *J. Am. Chem. Soc.*, 1989, **111**, 9177–9185.

36 T. R. Ward, O. Schafer, C. Daul and P. Hofmann, Geometry of Coordinatively Unsaturated Two-Legged Piano Stool Complexes with 16 Valence Electrons: A Theoretical Study, *Organometallics*, 1997, **16**, 3207–3215.

37 P. Hofmann, Unsaturated Organometallic Intermediates: Electronic Structure and Structural Dynamics of (η^5-C_5H_5)$Mn(CO)_2$, *Angew. Chem., Int. Ed. Engl.*, 1977, **16**, 536–537.

38 M.-D. Su and S.-Y. Chu, Theoretical Model for Insertion of the 16-Electron Species (η^5-C_5H_5)M(L) into Saturated Hydrocarbons. A (η^5-C_5H_5)M(CO) + CH_4 (M = Ru^-, Os^-, Rh, Ir, Pd^+, Pt^+) Case Study, *Organometallics*, 1997, **16**, 1621–1627.

39 M.-D. Su and S.-Y. Chu, An Energetically Feasible Mechanism for the Activation of the C–H Bond by the 16-Electron $CpM(PH_3)(CH_3)^+$ (M = Rh, Ir) Complex. A Theoretical Study, *J. Am. Chem. Soc.*, 1997, **119**, 5373–5383.

40 V. Gandon, N. Agenet, K. P. C. Vollhardt, M. Malacria and C. Aubert, Cobalt-Mediated Cyclic and Linear 2:1 Cooligomerization of Alkynes with Alkenes: A DFT Study, *J. Am. Chem. Soc.*, 2006, **128**, 8509–8520.

41 N. Agenet, V. Gandon, K. P. C. Vollhardt, M. Malacria and C. Aubert, Cobalt-Catalyzed Cyclotrimerization of Alkynes: The Answer to the Puzzle of Parallel Reaction Pathways, *J. Am. Chem. Soc.*, 2007, **129**, 8860–8871.

42 V. Gandon, N. Agenet, K. P. C. Vollhardt, M. Malacria and C. Aubert, Silicon–Hydrogen Bond Activation and Hydrosilylation of Alkenes Mediated by CpCo Complexes: A Theoretical Study, *J. Am. Chem. Soc.*, 2009, **131**, 3007–3015.

43 P. Hofmann and M. Padmanabha, Electronic and Geometric Features of (η^5-C_5H_5)ML 16-Electron Fragments. A Molecular Orbital Study of Ligand Effects, *Organometallics*, 1983, **2**, 1273–1284.

44 J. Song and M. B. Hall, Theoretical Studies of Inorganic and Organometallic Reaction Mechanisms. 6. Methane Activation on Transient Cyclopentadienylcarbonylrhodium, *Organometallics*, 1993, **12**, 3118–3126.

45 D. G. Musaev and K. Morokuma, Ab Initio Molecular Orbital Study of the Mechanism of H-H, C-H, N-H, O-H and Si-H Bond Activation on Transient Cyclopentadienylcarbonylrhodium, *J. Am. Chem. Soc.*, 1995, **117**, 799–805.

46 M. Couty, C. A. Bayse, R. Jiménez-Cataño and M. B. Hall, Controversial Exothermicity of the Oxidative Addition of Methane to (Cyclopentadienyl)rhodium Carbonyl, *J. Phys. Chem.*, 1996, **100**, 13976–13978.

47 P. E. M. Siegbahn, Comparison of the C−H Activation of Methane by M(C_5H_5)(CO) for M = Cobalt, Rhodium, and Iridium, *J. Am. Chem. Soc.*, 1996, **118**, 1487–1496.

48 M.-D. Su and S.-Y. Chu, A Theoretical Model for the Orientation of 16-Electron CpML Insertion into the C-H Bond of Propane and Cyclopropane and Its Regio- and Stereoselectivity, *Chem.–Eur. J.*, 1999, **5**, 198–206.

49 M.-D. Su and S.-Y. Chu, A New Aspect for the Insertion of the 16-Electron Species (η^5-C_5H_5)ML into Saturated Hydrocarbons. A (η^5-C_5H_5)ML + CH_4 (M = Rh, Ir; L = CO, SH_2, PH_3) Case Study, *J. Phys. Chem. A*, 1997, **101**, 6798–6806.

50 M. J. Frisch; G. W. Trucks; H. B. Schlegel; G. E. Scuseria; M. A. Robb; J. R. Cheeseman; G. Scalmani; V. Barone; B. Mennucci and G. A. Petersson*et al.*, Gaussian, Inc., Wallingford CT, 2013.

51 F. Weigend and R. Ahlrichs, Balanced Basis Sets of Split Valence, Triple Zeta Valence and Quadruple Zeta Valence Quality for H to Rn: Design and Assessment of Accuracy, *Phys. Chem. Chem. Phys.*, 2005, **7**, 3297–3305.

52 P. Hofmann, Unsaturated Organometallic Intermediates: Electronic Structure and Structural Dynamics of (η^5-C_5H_5)$Mn(CO)_2$, *Angew. Chem., Int. Ed. Engl.*, 1977, **16**, 536–537.

53 P. Hofmann and M. Padmanabhan, Electronic and Geometric Features of (η^5-C_5H_5)ML 16-Electron Fragments. A Molecular Orbital Study of Ligand Effects, *Organometallics*, 1983, **2**, 1273–1284.

54 T. R. Ward, O. Schafer, C. Daul and P. Hofmann, Geometry of Coordinatively Unsaturated Two-Legged Piano Stool Complexes with 16 Valence Electrons: A Theoretical Study, *Organometallics*, 1997, **16**, 3207–3215.

55 M. J. Bearpark, M. A. Robb and H. B. Schlegel, A Direct Method for The Location of The Lowest Energy Point on

a Potential Surface Crossing, *Chem. Phys. Lett.*, 1994, **223**, 269–274.

56 M.-D. Su, Model Study of The Photochemical Rearrangement Pathways of 1,2,4-Oxadiazole, *ChemPhysChem*, 2014, **15**, 2712–2722.

57 M.-D. Su, A Model Study on the Photochemical Isomerizations of Isothiazoles and Thiazoles, *Phys. Chem. Chem. Phys.*, 2014, **20**, 17030–17042.

58 M.-D. Su, A Theoretical Investigation of Photochemical Reactions of an Isolable Silylene with Benzene, *Chem.–Eur. J.*, 2014, **16**, 9419–9423.

59 M.-D. Su, A Model Study on The Photochemical Isomerizations of Cyclic Silenes, *Phys. Chem. Chem. Phys.*, 2015, **17**, 5039–5042.

60 M.-D. Su, Excited-State Photolytic Mechanism of Cyclopentene Containing A Group 14 Element: A MP2-CAS//CASSCF Study, *J. Phys. Chem. A*, 2015, **119**, 8611–8618.

61 M.-D. Su, A Mechanistic Study of the Addition of Alcohol to a Five-Membered Ring Silene *via* a Photochemical Reaction, *Phys. Chem. Chem. Phys.*, 2016, **18**, 8228–8234.

62 S.-H. Su and M.-D. Su, Mechanistic Investigations of CO-Photoextrusion and Oxidative Addition Reactions of Early Transition-Metal Carbonyls: $(\eta^5\text{-}C_5H_5)M(CO)_4$ (M = V, Nb, Ta), *Phys. Chem. Chem. Phys.*, 2016, **18**, 16396–16403.

63 Z.-F. Zhang, H.-C. Hua, S.-H. Su and M.-D. Su, Mechanistic Investigations on the Photorearrangement Reactions of $M(CO)_4(CS)$ (M = Group 6 Metal), *Inorg. Chem.*, 2016, **55**, 9017–9025.

64 M.-D. Su, Mechanistic Investigations of the Photochemical Isomerizations of $[(CO)_5MC(Me)(OMe)]$ (M = Cr, Mo, and W) Complexes, *ACS Omega*, 2017, **2**, 5395–5406.

65 Z.-F. Zhang and M.-D. Su, A Mechanistic Study for The Photochemical Reactions of d^6 $M(CO)_5(CS)$ (M = Cr, Mo, and W) Complexes, *ACS Omega*, 2017, **2**, 2813–2826.

66 J. P. Perdew, J. A. Chevary, S. H. Vosko, K. A. Jackson, M. R. Pederson, D. J. Singh and C. Fiolhas, Atoms, Molecules, Solids, and Surfaces: Applications of the Generalized Gradient Approximation for Exchange and Correlation, *Phys. Rev. B: Condens. Matter Mater. Phys.*, 1992, **46**, 6671–6687.

67 B. Metz, H. Stoll and M. Dolg, Small-Core Multiconfiguration-Dirac–Hartree–Fock-Adjusted Pseudopotentials for Post-d Main Group Elements: Application to PbH and PbO, *J. Chem. Phys.*, 2000, **113**, 2563–2569.

68 C. Lee, W. Yang and R. G. Parr, Development of the Colle-Salvetti Correlation-energy Formula into a Functional of the Electron Density, *Phys. Rev. B: Condens. Matter Mater. Phys.*, 1988, **37**, 785–789.

69 F. E. Jorge, A. C. Neto, G. G. Camiletti and S. F. Machado, Contracted Gaussian Basis Sets for Douglas–Kroll–Hess Calculations: Estimating Scalar Relativistic Effects of Some Atomic and Molecular Properties, *J. Chem. Phys.*, 2009, **130**, 064108–064113.

70 N. X. Wang and A. K. Wilson, Effects of Basis Set Choice upon the Atomization Energy of the Second-Row Compounds SO_2, CCl, and ClO_2 for B3LYP and B3PW91, *J. Phys. Chem. A*, 2003, **107**, 6720–6724.